# Computation of the Average and Harmonic Noise Power Spectral Density in Switched Capacitor Circuits

V.Vasudevan

Department of Electrical Engineering

Indian Institute of Technology-Madras

Chennai-600036, India

Email: vinita@ee.iitm.ernet.in

M.Ramakrishna

Department of Aerospace Engineering

Indian Institute of Technology-Madras

Chennai-600036, India

Email:krishna@aero.iitm.ernet.in

**Abstract**

Switched capacitor circuits are periodically time-varying circuits and the noise at the output of these circuits is cyclostationary. This noise is therefore characterized by the average and harmonic spectral densities. In this paper, we extend the method proposed in [1] to compute the average and harmonic noise spectral densities in periodically varying ciruits. We derive expressions for the average and harmonic spectral densities and use the mixed-frequency-time technique for the computation. The results for the average spectral density are compared with published results. The contribution of the harmonic spectral densities to the average noise spectral density at the output of a cascaded block is estimated.

**Keywords:** Circuit noise spectral density, simulation, analog circuits, switched capacitor circuits

## I. INTRODUCTION

Computation of noise spectral density in periodically varying circuits (and in particular, switched capacitor circuits) has received considerable attention over several decades. In 1970, Rice [2] obtained the noise spectral density of a periodically switched $RC$ circuit driven by white noise. He used an analytical expression for the time-varying impulse response. This method was later extended by Toth *et al* [3] to obtain power spectral density of noise in switched capacitor (SC) circuits. They solve for the sampled and held noise and continuous time or tracking noise seperately. This approach of splitting the noise into two parts has also been adopted in [4]. Instead of using series summations to take care of aliased noise, they numerically evaluate complex line integrals. A different approach was used by Goette *et al* [5], who solved the Lyapunov equation to get the time averaged autocorrelation. Using this along with the discretized z-domain equations of the network, they obtained the noise spectral density in switched capacitor circuits. In all three methods [3], [4], [5], the "full and fast charge transfer" approximation is used. This may not be completely valid in many of the circuits. A SPICE based approach has been proposed by Fisher [6]. He computed the noise spectral density by converting the SC circuit to an equivalent RC circuit and then using SPICE for the noise analysis. In order to take into account the aliased noise, he assumed knowledge of the noise bandwidth.

The average noise spectral density in linear periodically time varying (LPTV) circuits with

wide sense stationary (WSS) noise sources can be written as:

$$S(\omega) = \sum_{i=1}^{M} \sum_{n=-\infty}^{\infty} |H_n(\omega - n\omega_o)|^2 S_i(\omega - n\omega_o) \tag{1}$$

Here, $M$ represents the total number of noise sources in the circuit and the index $n$ is used for the aliasing sidebands. $H_n(\omega)$ represents the $n^{th}$ harmonic of the time-varying transfer function and $S_i(\omega)$ is the stationary power spectral density of the $i^{th}$ noise source. Many of the other methods proposed for SC circuits are efficient ways to compute equation (1). The adjoint network technique [7] has been used in [8], [9], [10], [11], [12], [13] to make the computation of noise due to several sources efficient. In addition, the frequency reversal properties of the adjoint network has been used in [12], [13] to reduce the number of transient simulations required to compute the effect of aliased noise. In [11], the mixed frequency time technique (MFT) [14], [15], [16], [17] was used along with Krylov subspace methods to make the computation of the transfer function efficient.

In LPTV circuits, the output noise is cyclostationary. It is more appropriately characterized by the instantaneous spectral density $S(t, \omega)$ [18], [19], which is a periodic function of time. Its description requires both the average and harmonic power spectral densities (HPSDs). Strom and Signell [20] obtained an expression for the instantaneous spectral density assuming stationary input noise sources. This was later extended to include cyclostationary noise sources by Roychowdhury *et al* [21]. They proposed an efficient harmonic balance based method to compute the average and the harmonic PSDs of noise.

The most general framework to compute the effects of white noise in any circuit in which noise can be regarded as a perturbation is the method based on stochastic differential equations (SDEs) [22], [23]. Demir *et al* [24] have used this method to get the time-varying covariance matrix in circuits. An algorithm to compute the average noise spectral density in time-varying circuits using the methodology of SDEs has been proposed in [1]. The main advantage of this method is that it can be used for all circuits, including oscillators where the phase noise is non-stationary. It can also be easily integrated into a standard circuit simulator such as SPICE. Both stationary and non-stationary noise sources can be included. Also, the effect of all noise sources can be considered simultaneously. A disadvantage of the method is that, since it is a time-domain technique, it is relatively expensive to include $1/f$ noise sources.

In this paper, we extend the algorithm proposed in [1] and develop a new technique to compute the average and harmonic spectral densities of noise in periodically time-varying circuits. We derive expressions for the average and harmonic spectral densities and use the mixed-frequency-time technique for the computation. The algorithm itself is applicable to all periodically varying circuits. In this paper, we have used it to compute the average and harmonic noise spectral density in switched capacitor circuits. Although there are several computations of the average spectral density, we are not aware of any computations done for the harmonic spectral densities in switched capacitor circuits. As pointed out in [21], both of these are required to build noise macromodels of time-varying circuits.

This paper is organized as follows. Section 2 summarizes the results of [1]. In Section 3, we derive expressions for the average and harmonic power spectral densities. Section 4 describes how the mixed-frequency-time technique can be used for the computation. In section 5, the application of the algorithm to the spectral density computation in switched capacitor circuits is discussed and section 6 contains the results.

## II. BACKGROUND

The state variable form of the circuit equations without noise sources can be written as:

$$\frac{d\mathbf{x}(t)}{dt} = \mathbf{F}(\mathbf{x}(t), \mathbf{v}(t)) \tag{2}$$

where $\mathbf{x}(t)$ is the vector containing the state variables of the circuit and $\mathbf{v}(t)$ is the vector of large signal excitations to the circuit. This can be solved to get the large signal steady state solution of the circuit, $\mathbf{x}_s(t)$.

With the noise sources added, the solution is assumed to be of the form:

$$\mathbf{x}(t) = \mathbf{x}_s(t) + \mathbf{x}_n(t)$$

where $\mathbf{x}_n(t)$ represents the noise voltages. Since noise is treated as a perturbation, a linearized form of the state equations along with additive noise sources can be used for noise computations. The large signal input sources are set to zero. The linearized equations can be written as:

$$\frac{d\mathbf{x}_n(t)}{dt} = \mathbf{A}(t)\mathbf{x}_n(t) + \mathbf{B}(t)\mathbf{u}(t) \tag{3}$$

In this set of equations, $\mathbf{A}(t)$ is the Jacobian of $\mathbf{F}(\cdot)$ computed at steady state. $\mathbf{B}(t)$ is a matrix containing the spectral intensity of the noise sources and $\mathbf{u}(t)$ is the vector containing the various noise sources, all of which are assumed to be standard Gaussian white noise processes uncorrelated with each other.

Assume that the noise spectral density is to be determined at node '$N$' of the circuit. Let $x_{nN}(t)$ be the noise waveform at this node. For convenience, it is assumed that $x_{nN}(t)$ is also a state variable. We define:

$$X_N(t;\omega) = \int_0^t x_{nN}(\tau)e^{-j\omega\tau}d\tau \tag{4}$$

$X_N(t;\omega)$ is essentially the Fourier transform of a "t-segment" of the noise waveform. The expected energy spectral density of this finite segment of the waveform, $\mathcal{E}(t;\omega)$, can be written as:

$$\mathcal{E}(t,\omega) = E\{|X_N(t;\omega)|^2\}$$

Here $E\{\cdot\}$ denotes the expectation operator.

Using the methodology of stochastic differential equations, it can be shown that the energy spectral density and the cross-spectral density, ($\mathbf{Y}(t;\omega)$), are given as [1]:

$$\frac{d\mathcal{E}(t;\omega)}{dt} = Y_N(t;\omega)e^{-j\omega t} + Y_N^*(t;\omega)e^{j\omega t} \tag{5}$$

$$\frac{d\mathbf{Y}(t;\omega)}{dt} = \mathbf{A}(t)\mathbf{Y}(t;\omega)(t) + E\{\mathbf{x}_n(t)x_{nN}^*(t)\}e^{j\omega t} \tag{6}$$

where $\mathbf{Y}(t;\omega)$ is a vector with:

$$Y_i(t;\omega) = E\left\{x_{ni}(t)X_N(t;\omega)^*\right\}$$

The second term in equation (6) is a vector containing the time-varying variance at the output node and its cross correlation with other nodes in the circuit. This can be obtained by solving the differential equations for the time-varying covariance matrix [24], [25], given as:

$$\frac{d\mathbf{K}(t)}{dt} = \mathbf{K}(t)\mathbf{A}(t)^{*T} + \mathbf{A}(t)\mathbf{K}(t) + \mathbf{B}(t)\mathbf{B}(t)^T \tag{7}$$

where

$$K_{ij}(t) = E\{x_{ni}(t)x_{nj}^*(t)\}$$

is the noise correlation matrix.

In order to obtain the average power spectral density of noise, equations (5), (6) and (7) need to be integrated in time until a steady state $S_o(\omega)$ is obtained. A more detailed derivation of the equations can be found in [1].

## III. Algorithm for Computation of the Average and Harmonic Spectral densities

Since SC circuits are periodically varying circuits, the output noise is cyclostationary (assuming that the circuit is stable). Therefore, the autocorrelation and power spectral density of the output noise are periodic functions of time. The circuit is thus characterized by an instantaneous power spectral density $S(t,\omega)$, which is periodic. However, the instantaneous power spectral density is essentially the time derivative of the (time-varying) energy spectral density [26]. Therefore, we can use equation (5) to get:

$$\begin{aligned} S(t,\omega) &= \frac{d\mathcal{E}(t;\omega)}{dt} \\ &= Y_N(t,\omega)e^{-j\omega t} + Y_N^*(t,\omega)e^{j\omega t} \end{aligned} \tag{8}$$

Since noise is regarded as a perturbation, the set of equations (7), for the covariance matrix, and (6), for the cross-spectral densities, are linear time-varying equations. Moreover, since both the input vector (consisting of the noise sources) and the state matrix vary periodically with the clock, the steady state covariance matrix is a periodic function of the clock. Therefore, each element of the covariance matrix can be expanded as a Fourier series in terms of the clock. This can be written as:

$$\mathbf{K}(t) = \sum_{k=-\infty}^{\infty} \mathbf{C}_k e^{jk\omega_o t} \tag{9}$$

Here, $\mathbf{C}_k$ is the matrix containing the $k^{th}$ Fourier coefficients of the elements of the covariance matrix. As mentioned previously, the second term in equation (6) is the $N^{th}$ column (or row, since $\mathbf{K}(t)$ is real and symmetric), $K_N(t)$, of the covariance matrix. It contains the variance of the output node and its cross-correlation with the other nodes in the circuit. Therefore,

$$\mathbf{K}_N(t) = \sum_{k=-\infty}^{\infty} \mathbf{C}_{kN} e^{jk\omega_o t} \tag{10}$$

Now, consider the set of equations for the cross-spectral densities, equation (6). These equations are also linear time-varying equations. However, they contain both the "measurement"

frequency $\omega$ (the frequency at which the spectral density is desired), and the clock frequency, $\omega_c$. The "input" vector in equation (6) is effectively a product of a tone at $\omega$ and the vector $\mathbf{K}_N(t)$. Therefore, using equation (10), the set of equations (6) can be written as:

$$\frac{d\mathbf{Y}(t;\omega)}{dt} = \mathbf{A}(t)\mathbf{Y}(t;\omega) + e^{j\omega t}\sum_{k=-\infty}^{+\infty}\mathbf{C}_{kN}e^{jk\omega_c t} \tag{11}$$

The solution $\mathbf{Y}(t;\omega)$ will therefore contain components at frequencies $\omega \pm n\omega_c$. Since the differential equations are linear, no other harmonics of $\omega$ will be generated. Therefore, $\mathbf{Y}(t;\omega)$ can be written as:

$$\mathbf{Y}(t;\omega) = e^{j\omega t}\sum_{k=-\infty}^{+\infty}\mathbf{d}_k(\omega)e^{jk\omega_c t} \tag{12}$$

i.e. it contains a tone at $\omega$ and several components at $n\omega \pm \omega_c$. The vector $\mathbf{d}_k(\omega)$ is the vector containing the Fourier coefficients of the cross-spectral densities at $\omega$.

From equation (8), it is seen that in order to compute the instantaneous spectral density, we require $Y_N(t;\omega)(= E\left\{x_{nN}(t)X_N(t;\omega)^*\right\})$. Using equation (12) we can substitute for $Y_N(t;\omega)$ in equation (8). This gives:

$$S(t,\omega) = \sum_{k=-\infty}^{\infty}(d_{kN}(\omega)e^{jk\omega_c t} + d^*_{kN}(\omega)e^{-jk\omega_c t}) \tag{13}$$

Therefore, the average power spectral density at $\omega$, $S_0(\omega)$, and the harmonic spectral densities $S_k(\omega)$ can be written as follows.

$$S_o(\omega) = d_{0N}(\omega) + d^*_{0N}(\omega) = 2Re(d_{0N}(\omega)) \tag{14}$$

$$S_k(\omega) = d_{kN}(\omega) + d^*_{-kN}(\omega) \tag{15}$$

Clearly, the instantaneous spectral density depends only on the Fourier components of $Y_N(t;\omega)$. Therefore, once we obtain the periodic steady-state value of $Y_N(t;\omega)$, we essentially have the instantaneous spectral density. This gives us a completely different technique to compute the average and harmonic spectral densities. Numerically, it requires only computations of periodic steady-state solutions for which there are efficient methods. These are dicussed in the next section. Since these methods are essentially based on transient analysis, they can be easily integrated into a standard circuit simulator. However, for large circuits it is not computationally as efficient as the method proposed in [21].

$S(t,\omega)$ is the derivative of the energy spectral density which is a real function. Therefore, it is also real. Hence, $S_k(\omega) = S^*_{-k}(\omega)$. Note that this algorithm directly gives the one-sided spectral density. This is because the "input" vector to equation (11) are elements of the covariance matrix, which contain the total power. If the two-sided average and harmonic spectral densities are desired, they may be obtained as:

$$S_o(\omega) = d_{0N}(\omega)$$

and

$$S_k(\omega) = d_{kN}(\omega)$$

Since $K_N(t)$ and $\mathbf{A}(t)$ are real, we have:

$$Y_N(t;\omega) = Y^*_N(t;-\omega)$$

This implies:

$$d_{kN}(\omega) = d^*_{-kN}(-\omega)$$

This is as expected.

It is important to consider the harmonics of the power spectral density when cyclostationary noise is input to another periodically varying system. In this case, these harmonics will mix with the clock frequency of the subsequent block and contribute to the average spectral density, $S_{x_o}$, at the output of the cascaded blocks, according to the following equation [21]:[1]

$$S_{x_o}(\omega) = \sum_{k,j} H_{-j+k}(\omega + (-k+j)\omega_c) S_j(\omega - k\omega_c) H_k^{*^T}(\omega - k\omega_c) \tag{16}$$

Clearly, the part of the harmonic spectral densities in and around the clock harmonics will alias back to the signal band.

In order to compute the average and harmonic spectral densities, we require Fourier coefficients $d_{kN}(\omega)$. An efficient method to compute the Fourier coefficients is discussed in the next section.

[1]To derive this we have used the definition of the two-dimensional Fourier transform given in [27], [20]. A slighty different definition was used in [21]. So the equations appear a little different.

## IV. METHOD OF SOLUTION

In order to compute the instantaneous spectral density, we require the periodic steady state covariance matrix and the cross-spectral densities. The set of equations (7) for the covariance matrix is periodic with the clock. There are no other frequencies in this set of equations. The shooting Newton method [28] can therefore be used very efficiently to get the periodic steady state covariance matrix. In order to get the cross-spectral density, we need to obtain the periodic steady-state solution of equation (11). This is a little more complicated since there are two frequencies $\omega$ and $\omega_c$. The two methods that can potentially be used in this case are the shooting Newton method and the mixed-frequency-time technique [14], [15], [16], [17]. The shooting-Newton technique is applicable to circuits with a periodic steady state response. In this method, starting with an initial guess for $\mathbf{Y}(0;\omega)$, the equations have to be integrated for a complete period of $\mathbf{Y}(t;\omega)$. After integration for one period, the state transition matrix can be used to get the correction to $\mathbf{Y}(0;\omega)$. Using these corrected values, the equations have to be integrated once more for a complete period to get the power spectral density. This period also depends on the relationship between the frequency $\omega$, at which the spectrum is desired and the clock frequency, $\omega_c$. Therefore, the computation of the noise spectrum using this method could mean long transient simulations. In fact, if the two frequencies are non-commensurate, the output is quasi-periodic [14], [15] and it is not possible to use the shooting Newton method. MFT can be used to circumvent some of these difficulties. In this method, the transient solution computed over a few selected clock cycles can be used to accurately construct the quasi-periodic output signal. This method has been demonstrated to be very efficient for computation of the steady state output signal as well as distortion in large switched capacitor filter circuits [29], [17]. We have tried both these methods to solve for the cross-spectral density. Some of the results of these computations have been presented by us in [30].

In the MFT technique, the signal $\mathbf{Y}(t;\omega)$ is sampled at the clock frequency to obtain a discrete signal that is independent of the clock fundamentals. The number of samples required depends upon the number of Fourier coefficients needed to represent the envelop. Since the envelop is a single tone, MFT can be used to solve the set of equations (11) very efficiently. If $\mathbf{Y}(t;\omega)$ is

sampled at $t = 0$ and $t = T_c(= 1/f_c)$, we get:

$$\mathbf{Y}(0;\omega) = \sum_{k=-\infty}^{+\infty} \mathbf{d}_k(\omega) \tag{17}$$

and this gives:

$$\mathbf{Y}(T_c;\omega) = e^{j\omega T_c}\mathbf{Y}(0;\omega) \tag{18}$$

If $\Phi(\mathbf{Y}(t_i;\omega), t_i, t_f)$ is the state transition function for the set of equations (11):

$$\mathbf{Y}(T_c;\omega) = \Phi(\mathbf{Y}(0;\omega), 0, T_c) \tag{19}$$

Equations (18) and (19) can be combined to obtain:

$$\mathbf{F} = \mathbf{Y}(0;\omega)e^{j\omega T_c} - \Phi(\mathbf{Y}(0;\omega), 0, T_c) = 0 \tag{20}$$

Since the differential equations for the cross-spectral densities are linear, the state transition function is a linear function of the initial state $\mathbf{Y}(0;\omega)$. The Newton method will therefore give the solution of equation (20) in a single step. In order to solve it, we need the Jacobian matrix $J$ given by:

$$\mathbf{J} = \frac{\partial \mathbf{F}}{\partial \mathbf{Y}(0;\omega)} = e^{j\omega T_c}\mathbf{I}_N - \frac{\partial \Phi}{\partial \mathbf{Y}(0;\omega)} \tag{21}$$

Here $\mathbf{I}_N$ denotes $N \times N$ identity matrix, $N$ being the total number of state variables. The second term in the above equation is the sensitivity matrix, $\mathbf{T}_\phi$. It can be obtained as explained in [28]. We have used the trapezoidal rule with time step control based on divided differences to perform the transient integration. The sensitivity matrix, $\mathbf{T}_\phi$ can then be written as:

$$\mathbf{T}_\phi = \prod_{i=1}^{M}(\mathbf{I}_N - 0.5h_i\mathbf{A}(t_i))^{-1}(\mathbf{I}_N + 0.5h_i\mathbf{A}(t_i - h_i)) \tag{22}$$

If the initial guess is assumed to be zero, the correct initial state is given by:

$$\mathbf{Y}(0;\omega) = (e^{j\omega T_c}\mathbf{I}_N - \mathbf{T}_\phi)^{-1}\mathbf{Y}(T_c;\omega) \tag{23}$$

Both $\mathbf{Y}(T_c;\omega)$ and $\mathbf{T}_\phi$ are obtained by integrating the set of differential equations (11) for one clock cycle. For $\omega = \omega_c$, MFT gives the same equation as the shooting Newton technique.

Once the corrected value of $\mathbf{Y}(0;\omega)$ is obtained, the power spectral density can easily be computed. The set of differential equations (11) have to be integrated once more for one clock

cycle using the corrected initial value of $\mathbf{Y}(0;\omega)$. The Fourier coefficients required for the average and harmonic spectral densities are computed as:

$$d_{0N}(\omega) = \frac{1}{T_c}\int_0^{T_c} Y_N(t;\omega)e^{-j\omega t}dt \tag{24}$$

$$d_{kN}(\omega) = \frac{1}{T_c}\int_0^{T_c} Y_N(t;\omega)e^{-j\omega t}e^{-jk\omega_c t}dt \tag{25}$$

Therefore, once the cross-spectral density at a particular frequency is obtained, computations of the average and harmonic spectral densities involve only additional integrations over a clock cycle.

Inspection of equation (11) reveals why this technique is very efficient for spectral density computations. Other than the clock fundamentals, $\mathbf{Y}(t;\omega)$ contains only the fundamental at $\omega$. As a result, the number of equations to be solved remains the same as the original set of differential equations. Moreover, as seen from equations (20) to (23), we only need to integrate the circuit equations over one clock cycle to get the corrected value of $\mathbf{Y}(0;\omega)$. Therefore, irrespective of $\omega$, the MFT method requires only two integrations of the circuit equations over a clock period to compute the instantaneous spectral density at a particular frequency. This is especially advantageous both for frequencies much smaller than the clock frequency and for frequencies very close to the clock frequency. In the first case, the envelop frequency is $\omega$ and in the second case it is $\omega - \omega_c$, both of which have an output period that is several times the clock period. Moreover, in the second case, the equations become very stiff since the components at $\omega$ and $\omega - \omega_c$ are of comparable magnitude and very small time steps have to be taken to get acceptable truncation error. Figure 1 shows the real and imaginary portion of $Y_N(t;\omega)$ obtained using the shooting Newton technique, for a switched capacitor bandpass filter with $f_c = 128kHz$ and $f = 123kHz$. In this case, the smallest output period that contains an integral number of cycles of all the frequencies is $1ms$. After $1ms$, the initial state is corrected and the integration is continued for one more period to obtain the spectral density. Besides the component at $f_c$ and $f$, it is clearly seen to contain the envelop at $5kHz$.

## V. Application to switched capacitor circuits

We have used the method described in section IV to compute the noise PSD in switched capacitor circuits. The state equations were derived directly for the simplified circuit. This gives

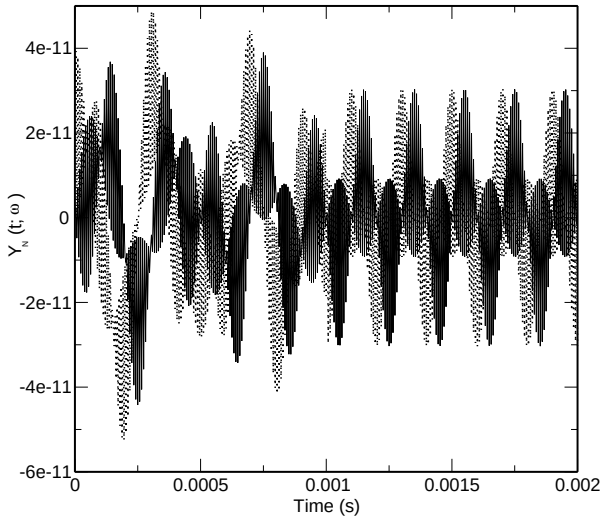


Fig. 1. Real and Imaginary portions of $Y_N(t;\omega)$ for $f_m = 123kHz$ and $f_c = 128kHz$. The initial state is corrected after 1ms.

a state matrix that is constant in each clock phase and varies periodically with the clock. In many of the switched capacitor circuits, the input to the operational amplifier has a capacitor cutset. A typical case is shown in Figure 2. As a result, the state equations turn out to be

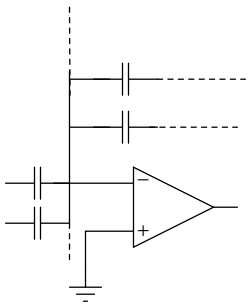


Fig. 2. Capacitor cutset in SC circuits

linearly dependent. This gives rise to numerical difficulties while solving for the covariance matrix. Usually, charge transfer relationships between capacitors are used to get a complete set of equations. These relationships can be converted to difference equations relating the various cross-correlations $K_{ij}(t)$ between nodes. This can be done as follows.

Assume that there are $N$ capacitor cutsets in the circuit. For each cutset, we can write a charge conservation equation. Let $\mathcal{A}_k$ represent one such cutset. It contains the set of capacitors that are related directly by the charge conservation equation. The conservation equation is written in

the form:

$$C_i\{V_i(t_2) - V_i(t_1)\} = \sum_{j\in\mathcal{R}_k} \alpha_j C_j\{V_j(t_2) - V_j(t_1)\},\ k = 1, 2, 3, \ldots, M \text{ and } i \in \mathcal{L}_k \tag{26}$$

The set $\mathcal{L}_k$ is in fact a singleton and $\mathcal{A}_k = \mathcal{L}_k \cup \mathcal{R}_k$. Effectively there are $M+1$ capacitors in this cutset. $V_i$ represents the voltage across the $i^{th}$ capacitor and $\alpha_i = \pm 1$ represents the sign of $V_i(t)$. If there are $N$ cutsets, $N$ such equations can be written.

In the following equations we use $\langle , \rangle$ to denote the expectation operator $E\{\cdot\}$. The variance of the voltage $V_i(t_2)$, $K_{ii}(t_2) = \langle V_i(t_2), V_i(t_2)\rangle$ can be evaluated as:

$$\begin{aligned} K_{i,i}(t_2) = K_{i,i}(t_1) - 2\sum_{j\in\mathcal{R}_k} \alpha_j \frac{C_j}{C_i} K_{i,j}(t_1) + \sum_{j\in\mathcal{R}_k}\sum_{l\in\mathcal{R}_k} \alpha_j\alpha_l \frac{C_jC_l}{C_i^2}\Big[K_{j,l}(t_2) + K_{j,l}(t_1)\Big] \\ +2\sum_{j\in\mathcal{R}_k} \alpha_j \frac{C_j}{C_i} \underbrace{\Big[\langle V_i(t_1), V_j(t_2)\rangle - \sum_{l\in\mathcal{R}_k} \alpha_l \frac{C_l}{C_i}\langle V_j(t_2), V_l(t_1)\rangle\Big]}_{A} \end{aligned} \tag{27}$$

Equation (27) contains terms of the form $K_{ij}(t_1, t_2)$, which need to be eliminated since the differential equations are derived for $K(t)$. This can be done as follows. Consider $i \in \mathcal{L}_k$ and $j \in \mathcal{R}_k$. $K_{ij}(t_2) = \langle V_i(t_2), V_j(t_2)\rangle$ can be written as:

$$K_{i,j}(t_2) = \sum_{l\in\mathcal{R}_k} \alpha_l \frac{C_l}{C_i} K_{l,j}(t_2) + \underbrace{\langle V_i(t_1), V_j(t_2)\rangle - \sum_{l\in\mathcal{R}_k} \alpha_l \frac{C_l}{C_i}\langle V_l(t_1), V_j(t_2)\rangle}_{B} \tag{28}$$

Substituting for $A$ in equation (27) by $B$ from equation (28), we get

$$K_{i,i}(t_2) - K_{i,i}(t_1) = \sum_{j\in\mathcal{R}_k} \alpha_j \frac{C_j}{C_i}\Big[K_{i,j}(t_2) - K_{i,j}(t_1)\Big] - \sum_{j\in\mathcal{R}_k}\sum_{l\in\mathcal{R}_k} \alpha_j\alpha_l \frac{C_jC_l}{C_i^2}\Big[K_{j,l}(t_2) - K_{j,l}(t_1)\Big] \tag{29}$$

Equation (29) is essentially a difference equation for the time evolution of the variance and can replace the corresponding ODE.

Each capacitor cutset will give rise to a similar equation. In addition, if there is more than one capacitor cutset, there will also be additional equations for the cross-correlation between capacitors. In order to derive the corresponding difference equations, consider two different cutsets $\mathcal{A}_p$ and $\mathcal{A}_q$. For $i \in \mathcal{L}_p$ and $j \in \mathcal{L}_q$ for $p \neq q$, we have:

$$\langle V_i(t_2), V_j(t_2)\rangle = \langle V_i(t_1) + \sum_{m\in\mathcal{R}_p} \alpha_m \frac{C_m}{C_i}\{V_m(t_2) - V_m(t_1)\}, V_j(t_1) + \sum_{n\in\mathcal{R}_q} \alpha_n \frac{C_n}{C_j}\{V_n(t_2) - V_n(t_1)\}\rangle \tag{30}$$

If equation (30) is expanded and terms are re-grouped, we get

$$\begin{aligned} K_{i,j}(t_2) = K_{i,j}(t_1) - \sum_{n\in\mathcal{R}_q} \alpha_n \frac{C_n}{C_j} K_{i,n}(t_1)\} - \sum_{m\in\mathcal{R}_p} \alpha_m \frac{C_m}{C_i} K_{j,m}(t_1) \\ + \sum_{m\in\mathcal{R}_p}\sum_{n\in\mathcal{R}_q} \alpha_m\alpha_n \frac{C_mC_n}{C_iC_j}\{K_{m,n}(t_2) + K_{m,n}(t_1)\} \\ + \sum_{m\in\mathcal{R}_p} \alpha_m \frac{C_m}{C_i} \underbrace{\left\{\langle V_j(t_1), V_m(t_2)\rangle - \sum_{n\in\mathcal{R}_q} \alpha_n \frac{C_n}{C_j}\langle V_m(t_2), V_n(t_1)\rangle\right\}}_{B} \\ + \sum_{n\in\mathcal{R}_q} \alpha_n \frac{C_n}{C_j} \underbrace{\left\{\langle V_i(t_1), V_n(t_2)\rangle - \sum_{m\in\mathcal{R}_p} \alpha_m \frac{C_m}{C_i}\langle V_m(t_1), V_n(t_2)\rangle\right\}}_{B} \end{aligned} \tag{31}$$

Once again, terms containing $K_{ij}(t_1, t_2)$ need to be eliminated. The last two expressions in the equation containing $K_{ij}(t_1, t_2)$ can be identified as $B$ of equation (27). Hence they can be eliminated using same the procedure as before. The equation for the cross-correlation can be obtained as:

$$\begin{aligned} K_{i,j}(t_2) - K_{i,j}(t_1) = \sum_{n\in\mathcal{R}_q} \alpha_n \frac{C_n}{C_j}\{K_{i,n}(t_2) - K_{i,n}(t_1)\} + \sum_{m\in\mathcal{R}_p} \alpha_m \frac{C_m}{C_i}\{K_{j,m}(t_2) - K_{j,m}(t_1) \\ - \sum_{m\in\mathcal{R}_p}\sum_{n\in\mathcal{R}_q} \alpha_m\alpha_n \frac{C_mC_n}{C_iC_j}\{K_{m,n}(t_2) - K_{m,n}(t_1)\} \end{aligned} \tag{32}$$

As is the case with the differential equations, if there are $N$ charge transfer equations in the switched capacitor circuit, there will be $\frac{(N)(N+1)}{2}$ equations for the time variation of the cross-correlations. These equations basically replace the corresponding differential equations.

## VI. RESULTS

We have obtained the noise spectrum in four switched capacitor circuits - a low pass and bandpass filter, a decimator and a parasitic insensitive integrator. The first three circuits are LPTV circuits for noise and the method proposed in this paper (described in section IV) has been used to get the average and harmonic noise spectral densities. The open loop integrator is a periodically switched circuit, but the output noise is non-stationary and not cyclostationary. This is because it is basically unstable, with a pole at zero frequency. The behaviour of the integrator

is similar to (linearized) oscillators and is described in more detail in [1]. The method adopted to get the noise spectral density of the integrator was slightly different and is described in more detail later.

The code was written in Python, a public domain scripting language. It was run on 1.7GHz Intel PIV processors running Linux. Within Python, the Numeric Python was used. We have assumed that the noise levels are independent of the signal levels. This is a good assumption for many of the commonly used switched capacitor circuits. We have also used simple linear macro-models for the switches and the operational amplifiers. Note that irrespective of the models used, the differential equations for noise computations are linear time-varying equations. Therefore, the efficiency of noise computations will not change if non-linear device models are used. The additional computation required would be to get the DC operating point. This is required for all algorithms proposed for noise spectral density calculations.

The first circuit was a switched capacitor low pass filter shown in Figure 3. Experimental were published by Toth *et al* [3] for this circuit. Closed switches are modelled using a resistance in parallel with a noise current source. The switch resistance is taken to be $80\Omega$. The operational amplifier is modelled using a voltage controlled voltage source with a finite bandwidth. It is assumed to have a unity gain frequency of $9\pi \times 10^6$rad/s and an ideal source follower output. In order to compare with published data, a white noise voltage source with a PSD of -61.5dB is connected to the non-inverting input of the opamp. The clock frequency is taken to be 4kHz. The capacitor values were taken to be $300pF$, $100pF$ and $100pF$ respectively. These are the values quoted by Toth *et al* [3]. For this circuit, experimental data is available upto three times

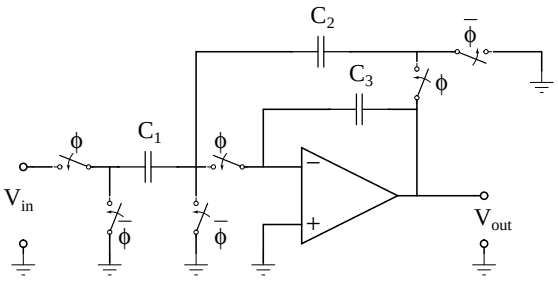


Fig. 3. Switched Capacitor low pass filter [3].

the clock frequency.

Figure 4 shows the average and the first three harmonics of the power spectral density. Also

included is the experimental data for the average spectral density published in [3]. The simulations of the average spectral density are seen to match well with experimental data. Both the shooting Newton and MFT give virtually identical results for the average power spectral density. The time taken by the two methods is shown in Table I. It is seen that MFT takes less than a fourth of the time taken by the shooting Newton technique.

The contributions to the average spectral density of a cascaded block will come from the region around the clock frequency and its harmonics. It is seen from Figure 4, that in these regions, HPSDs are comparable to the average spectral density and could contribute significantly. If we assume that we have an identical cascaded block, the contribution of the first harmonic spectral densities alone (j,k limited to $\pm 1$ in equation (16)) turns out to be about $5\%$ at $DC$.

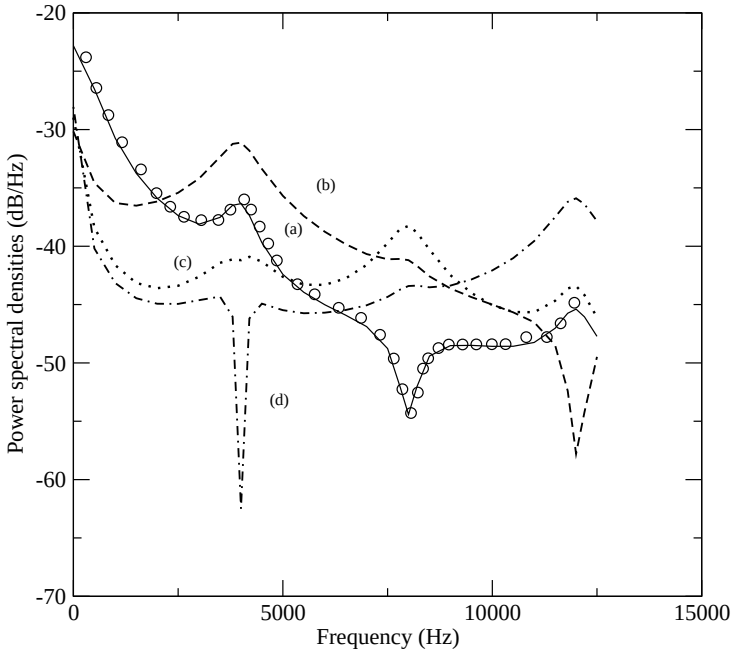


Fig. 4. Average and Harmonic Spectral densities of the lowpass filter. (a) is the average spectral density. (b),(c) and (d) are the first, second and third harmonic spectral densities. Circles indicate published experimental data [3].

The second circuit simulated was a bandpass filter shown in Figure 5. The output noise spectral density for this circuit has been computed in [31] and [13]. The clock frequency is 128kHz. The switches are modelled using a noisy $80\Omega$ resistor in series with an ideal switch. The input-referred white noise of the operational amplifier was assumed to be $20nV/\sqrt{(Hz)}$. The opamp was assumed to have infinite unity gain frequency. The values used are the same as those quoted in [13]. Published data for this circuit is available between 0 and 10kHz.

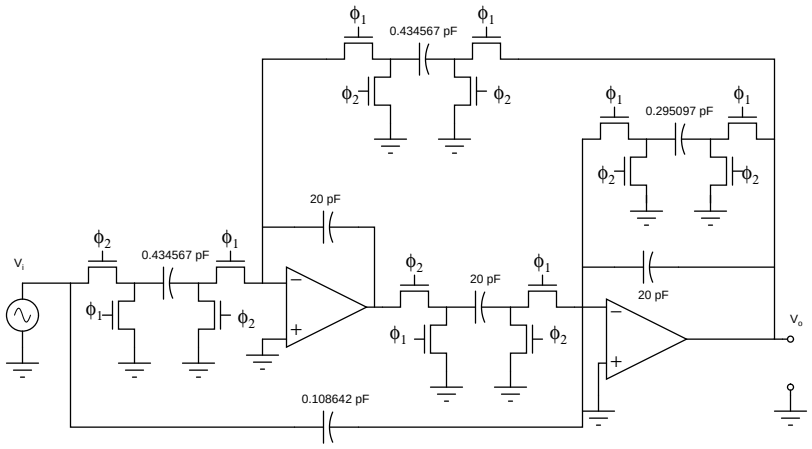


Fig. 5. Switched capacitor bandpass filter [31]

Figure 6 shows the average and harmonic spectral densities in this case. It is seen that the

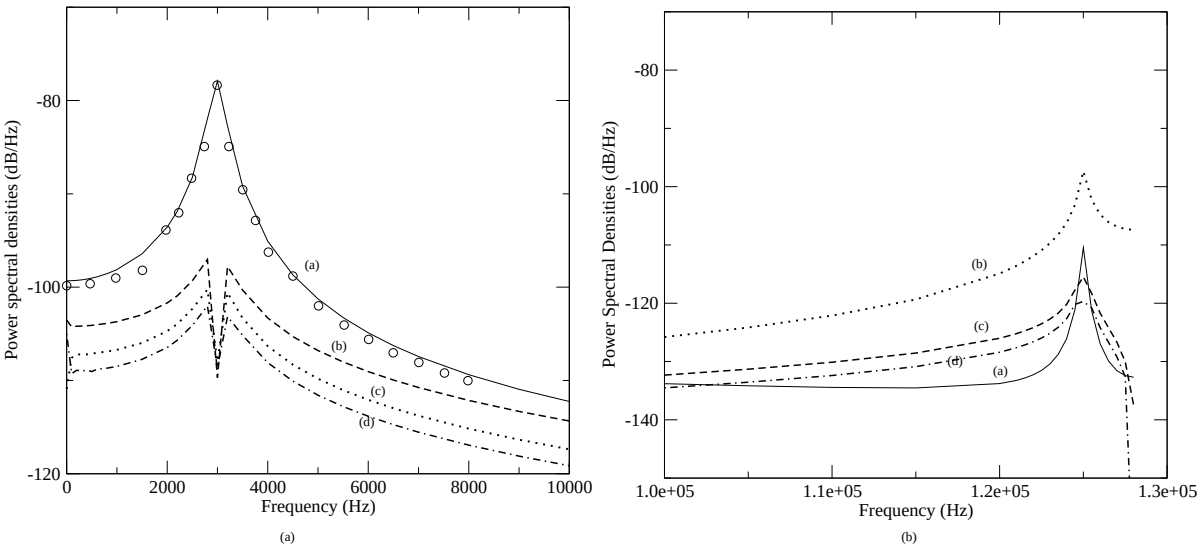


Fig. 6. Output noise spectral density of the bandpass filter. Circles indicate published data [31]. Curve (a) is the average spectral density and curves (b), (c) and (d) are the first, second and third harmonics of the noise spectral density.

average spectral density matches well with published data. Table I shows a comparison of the time taken using the shooting Newton and MFT techniques. As expected, the MFT technique is far more efficient. Direct integration of the equations takes more than a day. It should be noted that in the case of the shooting Newton technique, the time taken for computation depends strongly on the measurement frequency. For example, in the two cases simulated, it takes twice the amount of time to get the PSD at 0.5 kHz than at 1 kHz.

Figure 6(a) also shows the HPSDs in the signal band. Interestingly, for this circuit there is a sharp dip in the harmonic spectral densities at the point where the average spectral density peaks ($3kHz$). Also, the level of the HPSDs is about $30dB$ lower. It is therefore unlikely to make a significant change in the average spectral density at the output of a cascaded block. Figure 6(b) shows the average and harmonic spectral densities around the clock frequency. The levels here are also seen to be about $20dB$ lower. In fact, if an identical block is cascaded, the contribution of the first $HPSDs$ turns out to be negligible ( about $0.2\%$). In this case therefore, it is sufficient to use the average spectral density in the noise macromodel.

| Circuit | Method | Number of frequencies | Total time (seconds) | time/freq (seconds) |
|---|---|---|---|---|
| LPF | MFT | 26 | 464.42 | 17.86 |
| LPF | S-N | 28 | 2250.87 | 80.38 |
| BPF | MFT | 53 | 1011 | 19.07 |
| BPF | S-N | 54 | 45731 | 846.87 |
| Dec. | MFT | 33 | 761.42 | 23.07 |

TABLE I

COMPARISON OF THE TIME TAKEN BY SHOOTING NEWTON AND MFT.

The third circuit is a switched capacitor decimator [32] shown in figure 7. Here the clock frequency is 400KHz, but switches are controlled by clock phases that have different frequencies. The circuit itself is periodic, with a fundamental frequency corresponding to the lowest frquency. In the case shown, this is half the clock frequency. If MFT is used for the solution, the integration has to be done for one period of the lowest frequency clock, in this case 200KHz. The average and harmonic spectral densities for this case are shown in figure 8. The time taken is shown in table I.

The fourth example is the stray insensitive integrator shown in figure 9. The sample and held noise spectral density for this circuit has been computed in [4]. Here, the clock frequency is 26MHz and the amplifier DC gain and settling accuracy are 74dB and 80dB respectively. The values of the capacitances $C_1$, $C_2$ and $C_p$ are $1pF$, $2pF$ and $0.6pF$ respectively, as mentioned in [4].

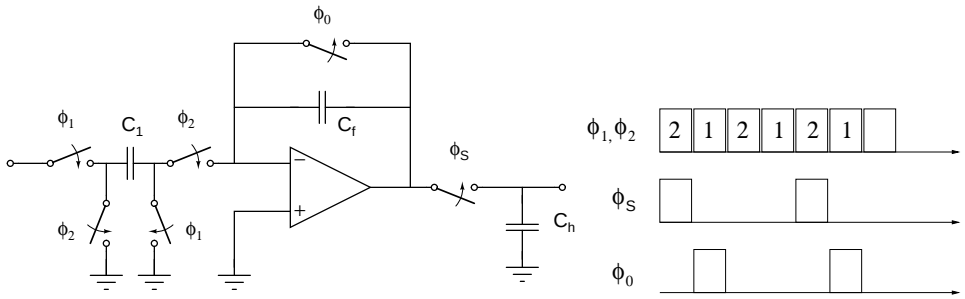


Fig. 7. Switched capacitor decimator [32]

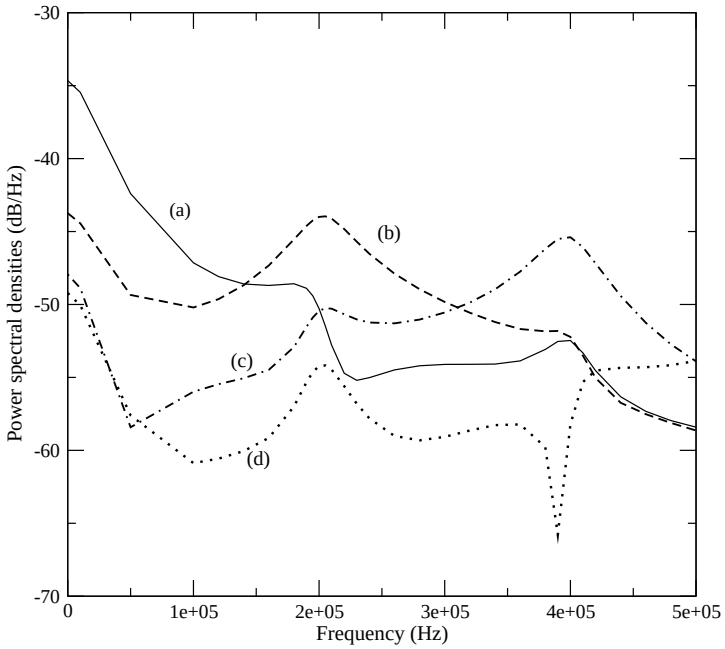


Fig. 8. Power spectral densities of the decimator. (a) is the average and (b), (c) and (d) are the first, second and third HPSD

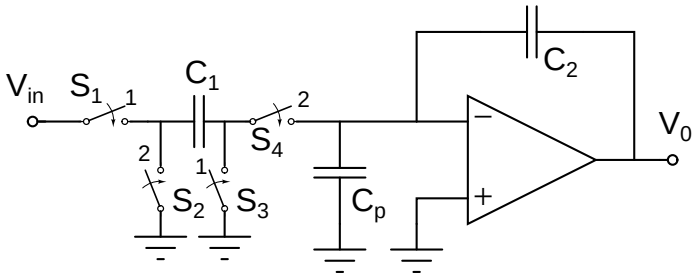


Fig. 9. Stray insensitive SC integrator [4].

As mentioned previously, the integrator has a pole at zero and is essentially unstable. As a result, the variance of noise at the output will keep increasing with time. This is shown in Figure 10(b). The output noise is nonstationary and not cyclostationary. However, as discussed in [1], the average noise spectral density can still be obtained. The computation was done as follows. The output noise variance was computed as a function of time and the results were stored in a table. This was then used for the transient analysis of equations (5) and (6), which were integrated until the steady state value for the average spectral density was obtained. The convergence behaviour is discussed in detail in [1].

Figure 10(a) shows a comparison of the computed results with the results published in [4]. The details of the OTA and switches are not given in the paper, but the noise due to the OTA and switches has been individually plotted. For our computations, we have adjusted the input referred noise of the OTA and the switch noise to match with this published data at 1 MHz. It can be seen that the computed results match reasonably well with published data over the entire frequency range. There is a slight discrepancy, which could be because in our case, the total noise is computed and not just the sample and held noise. It is not possible to seperate the sample and held noise and tracking noise in our method

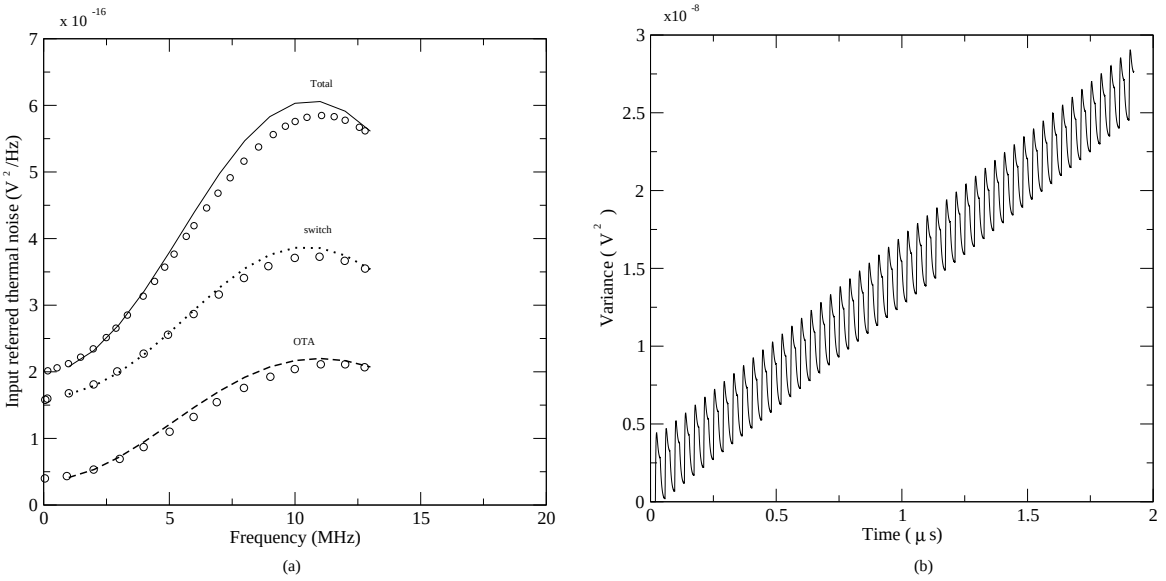


Fig. 10. (a) Average input referred noise spectral density of a stray insensitive SC integrator. The circles indicate published data [4] for sample and held noise. The three curves represent noise due to the OTA (dashed line), switches (dots) and the total noise (solid line). (b) Output noise variance as a function of time.

## VII. CONCLUSIONS

In this paper, we have proposed a new technique to compute the average and harmonic noise spectral densites in linear periodically varying circuits. The mixed frequency-time technique was used for the computation. Other than the method proposed in [21], this is the only method that can be used to compute the instantaneous spectral density. The method was demonstrated for switched capacitor circuits. The results of the average spectral density compare well with published data. In this method, the computation of harmonic spectral densities involves only additional integrations of the periodic steady state solution over a clock cycle. Note that, if the "input vector" in equation (11) is changed, the same code can also be used to get the transfer function and its harmonics. This is useful when we have a series of identical cascaded blocks (such as biquads). In these cases, a complete noise analysis can be done for a single circuit block and the average and harmonic noise spectral densities and the transfer funtions can be used to get the actual noise power spectral density at the output of the cascaded blocks.

## REFERENCES


[1] V.Vasudevan, "A time-domain technique for computation of noise spectral density in linear and non-linear time-varying circuits," *IEEE Trans. Circuits and Syst.-I*, vol. 51, pp. 422–433, Feb. 2004.

[2] S.O.Rice, "Response of periodically varying systems to noise-application to switched rc circuits," *Bell Syst. Tech. J.*, vol. 49, pp. 2221–2247, Nov. 1970.

[3] L.Toth, I.Yusim, and K.Suyama, "Noise analysis of ideal switched-capacitor networks," *IEEE Trans. Circuits and Syst.-I*, vol. 46, pp. 349–363, March 1999.

[4] O.Oliaei, "Numerical algorithm for noise analysis of switched-capacitor networks," *IEEE Trans. Circuits Syst - I*, vol. 50, pp. 865–876, July 2003.

[5] J.Goette and C.Gobet, "Exact noise analysis of sc circuits and an approximate computer implementation," *IEEE Trans. Circuits and Syst.*, vol. 3, pp. 508–521, April 1989.

[6] J.H.Fisher, "Noise sources and calculation techniques for switched capacitor filters," *IEEE J. Solid State Circuits*, vol. SC-17, pp. 742–752, Aug 1982.

[7] R.Rohrer, L.Nagel, R.Meyer, and L.Weber, "Computationally efficient electronic-circuit noise calculations," *IEEE J.Solid-State Circuits*, vol. SC-6, pp. 204–213, 1971.

[8] J.Vandewalle, H. D. Man, and J.Rabaey, "The adjoint switched capacitor network and its application to frequency,noise and sensitivity analysis," *Int. J.Circuit Theory Appl*, vol. 9, pp. 77–88, 1981.

[9] Z.Q.Shang and J.I.Sewell, "Efficient noise analysis methods for large nonideal sc and si circuits," in *Proc.IEEE ISCAS*, (Piscataway, NJ), pp. 565–568, 1994.

[10] M.Okumura, H.Tanimoto, T.Itakura, and T.Sugawara, "Numerical noise analysis for nonlinear ciruits with a periodic large signal excitation including cyclostationary noise sources," *IEEE Trans. Circuits and Syst.-I*, vol. 40, pp. 581–590, Sept. 1993.

[11] R.Telichevsky, K.Kundert, and J.White, "Efficient ac and noise analysis of two-tone rf circuits," in *Proc. IEEE DAC*, pp. 292–297, June 1996.

[12] F.Yuan and A.Opal, "Noise and sensitivity analysis of periodically switched linear circuits in frequency domain," *IEEE Trans. Circuits and Syst.-I*, vol. 47, pp. 986–998, July 2000.

[13] F.Yuan and A.Opal, "Adjoint network of periodically switched linear circuits with applications to noise analysis," *IEEE Trans. Circuits and Syst.-I*, vol. 48, pp. 139–151, Feb. 2001.

[14] L.O.Chua and A.Ushida, "Algorithms for computing almost periodic steady-state response of nonlinear systems to multiple input frequencies," *IEEE Trans. on Circuits and Systems*, vol. CAS-28, pp. 953–971, Oct. 1981.

[15] K. S. Kundert. and J. White and A. Sangiovanni-Vincentelli, "A Mixed Frequency-Time Approach for Finding the Steady-State Solution of Clocked Analog Circuits," in *Proceedings of the Custom Integrated Circuits Conference*, pp. 6.2.1–6.2.4, 1988.

[16] K. S. Kundert and J. White and A. Sangiovanni-Vincentelli, "A Mixed Frequency-Time Approach for Distortion Analysis of Switching Filter Circuits," *IEEE Journal of Solid-State Circuits*, vol. 24, pp. 443–451, Apr. 1989.

[17] D. Feng and J. Phillips and K. Nabors and K. Kundert and J. White, "Efficient computation of quasi-periodic circuit operating conditions via a mixed frequency / time approach," in *Proceedings of the Design Automation Conference*, pp. 635–640, 1999.

[18] W.A.Gardner, *Introduction to Random Processes:with applications to signals and systems*. New York: McGraw-Hill, 1989.

[19] M.T.Terrovitis, K.S.Kundert, and R.G.Meyer, "Cyclostationary noise in radio-frequency communication systems," *IEEE Trans. Circuits Syst. I*, vol. 49, pp. 1666–1671, Nov. 2002.

[20] T.Strom and S.Signell, "Analysis of periodically switched linear circuits," *IEEE Trans. Circuits Syst.*, vol. CAS-24, pp. 531–541, Oct. 1977.

[21] J.Roychowdhury, D.Long, and P.Feldmann, "Cyclostationary noise analysis of large rf circuits with multitone excitations," *IEEE J.Solid-State Circuits*, vol. 33, pp. 324–336, March 1998.

[22] C.W.Gardiner, *Handbook of Stochastic methods for Physics, Chemistry and the Natural Sciences*. New York: Springer-Verlag, 1983.

[23] B.Oksendal, *Stochastic Differential Equations*. Springer-Verlag, 5 ed., 1998.

[24] A.Demir, E.W.Y.Liu, and A.L.Sangiovanni-Vincentelli, "Time-domain non-monte carlo noise simulation for nonlinear dynamic circuits with arbitrary excitations," *IEEE Trans. Computer Aided Design*, vol. 15, pp. 493–505, May 1996.

[25] S. Shreve, "Lectures on stochastic calculus and finanace." www-2.cs.cmu.edu/ shreve/shreve.pdf.

[26] D.G.Lampard, "Generalization of the weiner-khintchine theorem to nonstationary processes," *J.Appl. Physics*, vol. 25, no. 6, pp. 802–803, 1952.

[27] A.Papoulis, *Probability, Random Variables and Stochastic Processes*. McGraw-Hill, 1965.

[28] T. Aprille and T. Trick, "Steady-State Analysis of Nonlinear Circuits with Periodic Inputs," *Proceeding of the IEEE*, pp. 108–114, Jan. 1972.

[29] J. Chen and S. Kang, "A Mixed Frequency-Time Approach For Quasi-Periodic Steady-State Simulation of Multi-Level Modeled Circuits," in *Proc. IEEE ISCAS*, pp. VI–194–197, 1999.

[30] V.Vasudevan and M.Ramakrishna, "Computation of noise spectral density in switched capacitor circuits using the mixed-frequency-time technique," in *Proc. IEEE DAC*, pp. 538–541, June 2003.

[31] L.Toth and K.Suyama, "Exact noise analysis of ideal swiched-capacitor networks," in *Proc. IEEE ISCAS*, pp. 1585–1588, June 1991.

[32] R.Unbehauen and A.Cichocki, *MOS Switched-Capacitor and Continuous-Time Integrated Circuits and Systems*. Springer-Verlag, 1989.